

# Fermi surface evolution in underdoped cuprates

Andrey V. Chubukov<sup>1,2</sup>, Dirk K. Morr<sup>1</sup> and Konstantin A. Shakhnovich<sup>3</sup>

<sup>1</sup>*Department of Physics, University of Wisconsin, Madison, WI 53706*

<sup>2</sup>*P.L. Kapitza Institute for Physical Problems, Moscow, Russia*

<sup>3</sup>*University of Chicago, Chicago, IL*

(today)

## Abstract

We consider a two-dimensional Fermi liquid coupled to low-energy commensurate spin fluctuations. At small coupling, the hole Fermi surface is large and centered around  $(\pi, \pi)$ . We show that as the coupling increases, the shape of the Fermi surface undergoes a substantial evolution, and at strong coupling, the hole Fermi surface consists of small pockets centered at  $(\pm\pi/2, \pm\pi/2)$ . At intermediate couplings, there exists a large hole Fermi surface centered at  $(\pi, \pi)$  as well as four hole pockets, but the quasiparticle residue is small everywhere except for the pieces of the pockets which face the  $\Gamma$  point. The relevance of these results to recent photoemission experiments in *YBCO* and *Bi2212* systems, and their relation to the Luttinger theorem are discussed.

A.C: It is a great pleasure to present a paper for a Festschrift in honor of David Pines. David's contributions to many fields in theoretical physics are well recognized throughout the world, as well as his charming personality. David, we wish you many more successful years in Many-Body Theory.

\*\*\*\*\*

The problem of fermions interacting with low-energy magnetic fluctuations has attracted a considerable interest over the past few years particularly in connection with high- $T_c$  superconductivity (Hertz 1976, Ioffe and Larkin 1989, Kampf and Schrieffer 1990, Ioffe and Kotliar 1990, Lee and Nagaosa 1992, Millis 1993, Monthoux and Pines 1994, Sachdev, Chubukov and Sokol 1995, Altshuler, Ioffe and Millis 1995, Sachdev and Georges 1995, Wen and Lee 1995). The vast majority of experimental results for cuprates indicate that the superconducting gap is highly anisotropic and its dominant part possesses  $d_{x^2-y^2}$  symmetry. The process which yields this kind of pairing is the exchange of nearly antiferromagnetic spin fluctuations. Photoemission experiments performed at optimal doping (Liu, Veal, Paulikas, Downey and Shi 1992, Liu, Veal, Paulikas, Downey, Kostic, Fleshler, Welp, Olson, Wu, Arko and Joyce 1992, Dessau, Shen, King, Marshall, Lombardo, Dickinson, Loeser, DiCarlo, Park, Kapitulnik and Spicer 1993, Ma, Quitmann, Kelley, Almeras, Berger, Margaritondo and Onnelion 1995) show that electrons possess a large, Luttinger-type Fermi surface whose area scales as  $1+x$  where  $x$  is the doping concentration. For this Fermi surface, D. Pines and Ph. Monthoux (Monthoux et al. 1994) have performed a number of strong coupling calculations of  $T_c$  within the Eliashberg formalism, and found  $T_c$  consistent with experiments.

There are however several issues related to the magnetic mechanism for superconductivity, which are still subjects of debates. Naively, one would expect that the magnetic mechanism should be the stronger, the closer the system is to the antiferromagnetic instability. Experimentally, however,  $T_c$  has a maximum at much larger doping concentrations than those where long-range magnetic order has been observed. Moreover, for a system with long-range order, one can study the electronic excitations and effective pairing interaction within the SDW technique (Schrieffer, Wen and Zhang 1989, Chubukov and Frenkel 1992).

At large Hubbard  $U$ , the ordered state possesses two bands of quasiparticles with  $Z \approx 1/2$  separated by a gap,  $2\Delta \approx U$ . Near half-filling, the valence band is nearly fully occupied, and the conduction band is empty. Accordingly, the hole Fermi surface has a *small* area which scales as  $x$  rather than  $1+x$ . The photoemission studies of  $Sr_2CuO_2Cl_2$  (Wells, Shen, Matsuura, King, Kastner, Greven and Birgeneau 1995) have demonstrated that the valence band maxima are at  $(\pi/2, \pi/2)$  and symmetry related points. This is consistent with the theoretical studies which yield hole pockets at  $(\pm\pi/2, \pm\pi/2)$  near half-filling. For this kind of Fermi surface, there are simply no low-energy quasiparticles in the directions of momentum space, where the  $d_{x^2-y^2}$  gap has the largest amplitude. Moreover, the interaction vertex between fermions and spin fluctuations obeys the Adler principle, i.e., it vanishes when the magnon momentum equals  $(\pi, \pi)$ . As a result, the full scattering potential between fermions, mediated by the exchange of spin fluctuations, does not have a peak at  $(\pi, \pi)$  and therefore one cannot get  $d_{x^2-y^2}$  pairing from the magnetic mechanism (Schrieffer 1994).

In a mean-field SDW approach, the gap,  $2\Delta$ , between conduction and valence bands is proportional to the sublattice magnetization, i.e., it vanishes when long-range order disappears. However, this is actually an artifact of the mean-field treatment. The easiest way to see this is to switch on a small, but finite temperature and compute lowest-order temperature corrections to the mean-field formulae. The corrections to the sublattice magnetization are logarithmically divergent which is an obvious consequence of the Mermin-Wagner theorem. At the same time, the divergent terms in the corrections to  $\Delta$  are cancelled out. As a result, at finite  $T$ ,  $2\Delta$  remains approximately equal to  $U$ , while the sublattice magnetization vanishes. This result is expected in some sense because the existence of two narrow bands with quasiparticle residue  $Z \approx 1/2$ , separated by an energy gap  $U$ , is similar to what one obtains by just considering the atomic limit of the Hubbard model near half-filling. From this perspective, the role of strong antiferromagnetic fluctuations is to transform the two

Hubbard levels into *coherent* bands of quasiparticles <sup>1</sup>.

The consideration above indicates that one can obtain an “almost” SDW description of the electronic states, with  $2\Delta \approx U$ , even without long-range order. This is consistent with QMC studies (Bulut, Scalapino and White 1994, Preuss, Hanke and von der Linden 1995) which show that the density of states in a paramagnetic phase near half-filling has two distinct peaks roughly separated by  $U$ . However, as the system moves away from half-filling, the spectral weight transfers from the upper band into the lower band, and near optimal doping there exists just one coherent band of quasiparticles. This implies that the features of an SDW solution appear gradually as the system moves from optimal doping to half-filling.

In the present paper, we analyse how the system acquires the properties of the SDW solution. We consider a simple model in which electrons are coupled to strong antiferromagnetic fluctuations by

$$\mathcal{H}_{int} = g \sum_{k,q,\alpha,\beta} c_{k+q,\alpha}^\dagger \vec{\sigma}_{\alpha,\beta} c_{k,\beta} \vec{S}_q \quad (1)$$

where  $g$  is the coupling constant, and  $\sigma_i$  are the Pauli matrices. We assume that the weak-coupling limit describes optimal doping and model the system’s evolution towards half-filling by increasing the strength of the coupling constant  $g$ . The partial justification for this assumption follows from the diagrammatic consideration of the near atomic limit of the Hubbard model which will be presented elsewhere. We will also assume that the original  $SU(2)$  symmetry is extended to  $SU(N)$ , substitute Pauli matrices by  $N^2 - 1$  traceless  $SU(N)$  generators, and perform the calculations for  $N \rightarrow \infty$ . In this limit, the mean-field SDW description becomes exact. Finally, we will assume that the dynamical spin susceptibility,  $\chi(q, \omega)$  is peaked at  $Q = (\pi, \pi)$  and its low-energy part has the form  $\chi_{ii}^{-1}(q, i\omega_m) = A^{-1}(\delta^2 +$

---

<sup>1</sup>Without strong magnetic fluctuations, the two bands which emerge from the Hubbard levels are likely to be mostly incoherent, and there also appears, at finite  $t$ , a coherent band at about  $U/2$ . This result was found in infinite- $D$  studies of the Hubbard model (Rozenberg, Kotliar, Kalueter, Thomas, Rapkine, Honig and Metcalf 1995).

$v_s^2(q - Q)^2 + \omega_m^2 + 2\gamma|\omega_m|$ ). We will consider  $\delta$  as a parameter which does not vary with the coupling strength. As a further simplification, we will assume that this form of the susceptibility holds when  $v_s|q - Q|$  and  $|\omega|$  are both smaller than some cutoff scale,  $C \ll W$ , where  $W$  is the fermionic bandwidth. At higher energy scales, we simply set  $\chi_{ii}(q, \omega) = 0$ . This sharp cutoff however is only used here to simplify the calculations - we will see that in order to obtain a strong Fermi surface evolution with increasing  $g$  we only have to assume that the spin susceptibility gets substantially reduced at the scales which are larger than  $W$ . The overall factor  $A$  is determined from  $\int d\vec{q}d\omega \chi_{ii}(q, \omega) = \hat{S}^2/(N^2 - 1)$ .

We now proceed to the calculations of the quasiparticle self-energy. We will first present the results for  $\gamma = 0$  when a full analytical calculation is possible, and then show how the results are modified due to finite damping.

The second-order self-energy contains the Green function of an intermediate state with momentum  $k + q$ . Since  $C \ll W$ , we can expand the fermionic energy  $\epsilon_{k+q}$  as  $\epsilon_{k+q} \approx \epsilon_{k+Q} + \vec{v}_{k+Q}\vec{q}$ , where  $\vec{q} = q - Q$ . Within this approximation, we obtained the analytical expression for  $\Sigma(k, \Omega)$  for arbitrary ratio of  $a_k = |v_{k+Q}|/v_s$ . It turns out, however, that the mechanism of the Fermi surface evolution is virtually insensitive to the value and momentum dependence of  $a_k$ . The results for arbitrary  $a_k$  will be presented in a separate publication, here we just set  $a_k = 1$  in which case the expression for the self-energy has the simple form <sup>2</sup>

$$\Sigma(k, \Omega_m) = -g_e^2 \frac{1}{\bar{\epsilon}_{k+Q} - i\Omega_m} \quad (2)$$

for  $\bar{\epsilon}_{k+Q}^2 + \Omega_m^2 \geq C^2$ , and

$$\Sigma(k, \Omega_m) = -g_e^2 \frac{1}{\bar{\epsilon}_{k+Q} - i\Omega_m} \frac{\sqrt{\bar{\epsilon}_{k+Q}^2 + \Omega_m^2 + \delta^2} - \delta}{\sqrt{C^2 + \delta^2} - \delta} \quad (3)$$

---

<sup>2</sup>In performing the integration, we actually set  $\vec{v}_{k+Q} = v_{k+Q}^x$ , integrated over  $\bar{q}_y$  from  $-\infty$  to  $+\infty$  and over the circle  $v_{k+Q}^2 \bar{q}_x^2 + \omega_m^2 < C^2$ . However, we also checked that the results change very little if we also restrict the integration over  $\bar{q}_y$  to  $|v_{k+Q}\bar{q}_y| < C$ .

for  $\bar{\epsilon}_{k+Q}^2 + \Omega_m^2 < C^2$ . Here we defined  $\bar{\epsilon}_k = \epsilon_k - \mu$ , and  $g_e = (2/N)^{1/2}g|\hat{S}|$ . The location of the Fermi surface follows from  $G^{-1}(k, 0) = -(\bar{\epsilon}_k + \Sigma(k, 0)) = 0$ .

The relevant issue for our consideration is how the chemical potential  $\mu$  changes with  $g_e$ . The value of  $\mu$  is obtained from the condition that  $2 \int d\vec{k}d\omega G(k, \omega) = N/V$ . We solved this equation numerically and present the result in Fig. 1. We found that  $\mu$  remains nearly the same as for free particles roughly up to  $g_e = g_3^{(3)}$ , when pockets are formed (see below), and then starts growing and approaches  $g_e$  at large couplings.

It is instructive to consider the large  $g_e$  limit in more detail. As  $|\mu|$  is large in this limit, the condition  $\Omega_m^2 + \bar{\epsilon}_{k+Q}^2 > C^2$  is satisfied for all momenta and Matsubara frequencies (though not for all real frequencies!), and the self-energy is given by (2). For the full Green function we then immediately obtain

$$G(k, \Omega_m) = \frac{i\Omega_m - \bar{\epsilon}_{k+Q}}{(i\Omega_m - E_1(k))(i\Omega_m - E_2(k))}, \quad (4)$$

where  $E_{1,2}(k)$  are given by

$$E_{1,2}(k) = \frac{\bar{\epsilon}_{k+Q} + \bar{\epsilon}_k}{2} \pm \left( g_e^2 + \left( \frac{\bar{\epsilon}_{k+Q} - \bar{\epsilon}_k}{2} \right)^2 \right)^{1/2}. \quad (5)$$

Performing now an analytical continuation to real frequencies, we find that the full Green function has two poles at  $\Omega = E_{1,2}(k) \approx |\mu| \pm g_e$ . It is easy to check that for both solutions the condition for using (2) for the self-energy (which, for real frequencies, is,  $|\Omega^2 - \bar{\epsilon}_{k+Q}^2| > C^2$ ) is satisfied. These two solutions obey  $E_{1,2}(k) = E_{1,2}(k+Q)$  and have exactly the same form as the mean-field solutions of the ordered SDW state with the effective coupling  $g_e$  playing the role of the SDW gap,  $\Delta$ . This exact equivalence with the SDW formulae is indeed the result of restricting with only the leading terms in the expansion in  $C/g_e$  - in the absence of a broken symmetry,  $k$  and  $k+Q$  are *not* equivalent points in the Brillouin zone, and in this sense, the quasiparticle bands at  $E_{1,2}$  are only the precursors of the conduction and valence bands of the ordered state. Further, it follows from (4) that the quasiparticle residue for each of these two solutions is  $Z = 1/2 + O(t/g_e)$ . Clearly then, the hole Fermi surface is small and encloses the area which scales as  $x$  rather than  $1+x$  as was the case for small  $g_e$ .

We now present our results for the Fermi surface evolution with varying  $g_e$  (Fig. 2). We found that the evolution begins with the “hot spots”, where  $\bar{\epsilon}_k = \bar{\epsilon}_{k+Q} = 0$ . It is clear from (3) that as  $\Sigma(\bar{\epsilon}_{k+Q} = 0, \Omega = 0) = 0$ , the location of the “hot spots” is not shifted by self-energy corrections. However, at  $g_e = g_e^{(1)} = (2\delta(\sqrt{C^2 + \delta^2} - \delta))^{1/2}$ , the Fermi velocity at these points turns to zero. At  $g_e > g_e^{(1)}$ , each of the “hot spots” is split into three: one is still at  $\bar{\epsilon}_k = 0$ , while the other two are located at  $\bar{\epsilon}_k = \pm(g_e^2/(\sqrt{C^2 + \delta^2} - \delta))(1 - (g_e^{(1)}/g_e)^2)^{1/2}$  at  $g_e < C$ , and at  $\bar{\epsilon}_k = \pm g_e$  when  $g_e > g_e^{(2)} = C$  (Fig. 2b). Besides, at  $g_e > g_e^{(2)}$ , there appear (for  $a_k = 1$ ) nested pieces of the Fermi surface located between points  $D$  and  $D'$  in Fig. 2c. For  $g_e$  only slightly larger than  $g_e^{(2)}$ , both  $D$  and  $D'$  are located near the magnetic Brillouin zone boundary. As  $g_e$  increases further, these points move apart and approach the Brillouin zone diagonal. Finally, at  $g_e = g_e^{(3)} = C(1 + 8t(|\mu| - C)/C)/(2t + \sqrt{4t^2 - 4|t|(|\mu| - C)})$ , the  $D$  and  $D'$  points from neighboring “hot spots” merge and the system undergoes a topological transition when the singly-connected hole Fermi surface splits into hole pockets centered at  $(\pm\pi/2, \pm\pi/2)$  and the large hole Fermi surface (Fig. 2d). As  $g_e$  increases further, the large Fermi surface shrinks (Fig. 2e) and eventually disappears, and at even larger  $g_e$ , the Fermi surface consists of just four hole pockets (Fig. 2f).

We further discuss how the quasiparticle residue along the Fermi surface changes with the coupling strength. At small  $g_e$ , the residue is nearly  $k$ -independent and is close to  $Z = 1$ . At large  $g_e$ ,  $Z$  along the hole pockets is again  $k$ -independent and is approximately equal to  $1/2$ . At intermediate  $g_e$ , however, we found a strong momentum dependence of  $Z$ . In Fig. 2e we present our results for  $Z$  when large and small Fermi surfaces coexist. We see that the quasiparticle residue along the large Fermi surface is very small which makes its experimental observation problematic. The residue along the hole pocket is also very anisotropic and is relatively close to 1 only in a momentum region which faces the  $\Gamma$  point. This is consistent with the experimental observations by R. Liu et al. who reported a small Fermi surface in  $YBa_2Cu_3O_{6.3}$ , but could only detect the Fermi surface crossing between the  $\Gamma$  and  $(\pi/2, \pi/2)$  points (Liu et al. 1992).

We now discuss how the results above change when we include the damping of spin

fluctuations. We found that the general scenario of the Fermi surface evolution does not change, but the value of  $g_e^{(1)}$  where each “hot spots” splits into three is in fact substantially larger than in the absence of damping. Specifically, we found (still, assuming for simplicity that  $a_k = 1$ ) that  $g_e^{(1)}(\gamma) = g_e^{(1)}(\gamma = 0)\Psi(\gamma/\delta)$  where  $\Psi(x) = 1 + x/(3\pi) + O(x^2)$  for  $x \ll 1$ , and  $\Psi(x) = (16 \log x/(\pi x))^{-1/2}$  for  $x \gg 1$ . Near optimal doping (which corresponds to weak/intermediate couplings in our consideration), spin fluctuations are overdamped, i.e.,  $\gamma \gg \delta$ . In this case,  $g_e^{(1)} \propto (\gamma C/\log \gamma/\delta)^{1/2}$  which is substantially larger than  $g_e^{(1)} \propto (\delta C)^{1/2}$  which we obtained in the absence of damping. Though the actual numbers depend on the details of the band structure and specific predictions about  $v_s$ , etc, it is essential that this critical value *does not* contain  $\delta^{1/2}$  as an overall factor.

Now about vertex corrections. We performed the same lowest-order computations as for the self-energy. At small and moderate  $g_e$ , the result strongly depends on the momenta of the external particles. In particular, it has been shown (Altshuler et al. 1995, Chubukov 1995) that if we set the momentum in the spin propagator  $q = Q$ , and choose the incoming and outgoing fermions to be right at the original “hot spots” (such that both fermions are simultaneously at the Fermi surface), then vertex corrections in fact *increase* the pairing potential and favor  $d$ -wave pairing. However, if we choose fermions to be at the new “hot spots” which appear at  $g_e > g_e^{(1)}$ , then the vertex corrections have opposite sign and decrease the pairing potential. At large  $g_e$ , only a single new “hot spot” survives. In this limit, we found (for  $a_k = 1$  and to leading order in  $C/g_e$ ) that the full vertex function is

$$g_e^{full}(k, \Omega_m) = g_e \frac{(i\Omega_m - E_1(k))(i\Omega_m - E_2(k))}{(i\Omega_m - \bar{\epsilon}_k)(i\Omega_m - \bar{\epsilon}_{k+Q})} \quad (6)$$

where  $E_{1,2}$  are given by (5). This form of the vertex function is the same as in the mean-field SDW solution for the ordered state. An analytical continuation of (6) to real frequencies requires care as (6) is valid only when  $|\Omega^2 - \bar{\epsilon}_k^2| > C^2$  and  $|\Omega^2 - \bar{\epsilon}_{k+Q}^2| > C^2$ . At  $\Omega = E_{1,2}(k)$ , these two conditions are satisfied, and we see that the full vertex function vanishes at resonance. Indeed, in the absence of the symmetry breaking, vanishing of  $g_e^{full}$  is again a result of neglecting the subleading terms. Nevertheless, we see that at  $g_e \gg C$ , vertex



corrections substantially reduce the effective pairing potential between fermions mediated by the exchange of spin fluctuations.

Now consider higher-order diagrams. Here the key point is that at large  $g_e$ , our results are the same as in the SDW description. Meanwhile, we found that the full mean-field SDW solution is given by the second-order self-energy diagram. Higher-order terms do not contribute because of a precise cancellation (at  $n \rightarrow \infty$ ) between self-energy and vertex corrections to the second-order self-energy term. In our case SDW solutions are reproduced only to lowest-order in  $C/g_e$ , i.e. there is no complete cancellation. However, the higher-order self-energy terms are still small, at  $g_e \gg C$ , compared to the second-order self-energy and can be neglected. At intermediate  $g_e \sim C$ , the restriction with only the second-order diagram is, strictly speaking, unjustified, but we expect that the scenario for the Fermi surface evolution will remain at least qualitatively the same as the one described above.

Finally, some considerations on the Luttinger theorem. It is clearly violated at large  $g_e$ . The source of this violation will be discussed in a separate publication, here we only notice that the key point of the Luttinger theorem is the proof, order by order in perturbation theory, that  $I = \int d\vec{k}d\Omega G(k, \Omega) d\Sigma(k, \Omega)/d\Omega = 0$ . Meanwhile, for the SDW state,  $I$  is actually finite, though a formal application of Luttinger's reasoning still yields  $I = 0$  to all orders in perturbation theory. The point is that the nonzero contribution to  $I$  comes solely from the region of  $(k, \Omega)$  where the Luttinger expansion parameter  $\Lambda = \Delta^2 |G_0(k, \Omega)G_0(k + Q, \Omega)| > 1$ , and perturbation series do not converge. We computed  $I$  and also the area of the Fermi surface with our self-energy. The results for the Fermi surface area are presented in Fig. 1b. Though at intermediate  $g$ , higher-order diagrams cannot be neglected and we cannot exactly reproduce the Luttinger theorem even when it should be valid, our numerical data indicate that the area stays nearly the same as for free fermions roughly up to  $g_e^{(3)}$  when the hole pockets get separated from the rest of the Fermi surface. We believe, though at the moment have no proof, that the Luttinger theorem ceases to work above  $g_e^{(3)}$ .

It is our pleasure to thank S. Chakravarty, E. Dagotto, A. Finkelstein, D. Frenkel, L. Ioffe, R. Joynt, A. Kampf, R. Laughlin, A. Moreo, P. Lee, A. Millis, M. Onellion, D. Pines,

A. Ruckenstein, S. Sachdev, D. Scalapino, B. Shraiman, A. Sokol and Q. Si for numerous discussions and comments. A.C. is an A.P. Sloan fellow.

## References

1. B. L. Altshuler, L. B. Ioffe, and A. J. Millis, preprint
2. N. Bulut, D. J. Scalapino, and S. R. White, Phys. Rev. Lett. **73**, 748 (1994)
3. A. V. Chubukov and D.M.Frenkel, Phys. Rev. B **46**, 11884 (1992)
4. A. V. Chubukov, Phys. Rev. B **52**, R3847 (1995)
5. D.S. Dessau, Z.-X. Shen, D. M. King, D. S. Marshall, L. W. Lombardo, P. H. Dickinson, A. G. Loeser, J. DiCarlo, C.-H. Park, A. Kapitulnik, and W. E. Spicer, Phys. Rev. Lett. **71**, 2781 (1993)
6. J.A. Hertz, Phys. Rev. B **14**, 1165 (1976)
7. L.B. Ioffe and A.I. Larkin, Phys. Rev. B **39**, 8988 (1989)
8. L.B. Ioffe and G. Kotliar, Phys. Rev. B **42**, 10348 (1990)
9. L.B. Ioffe, V.Kalmeyer and P.B. Wiegmann, Phys. Rev. B **43**, 1219 (1991)
10. L.B. Ioffe and A. Millis, preprint
11. A.P. Kampf and J.R. Schrieffer, Phys. Rev. B **42**, 7967 (1990)
12. C. Kane, P. Lee and N. Read, Phys. Rev. **39**, 6880 (1989)
13. P.A.Lee and N. Nagaosa, Phys. Rev. B **46**, 5621 (1992)
14. R. Liu, B. W. Veal, A. P. Paulikas, J. W. Downey, and H. Shi, Phys. Rev. B **45**, 5614 (1992)
15. R. Liu, B. W. Veal, A. P. Paulikas, J. W. Downey, P. J. Kostic, S. Fleshl er, U. Welp, C. G. Olson, X. Wu, A. J. Arko, and J. J. Joyce, Phys. Rev. B **46**, 11056 (1992)

16. Jian Ma, C. Quitmann, R. J. Kelley, P. Almeras, H. Berger, G. Margaritondo, and M. Onnellion, Phys. Rev. B **51**, 3832 (1995); Jian Ma, P. Almeras, R. J. Kelley, H. Berger, G. Margaritondo, X. Y. Cai, Y. Feng, and M. Onellion, Phys. Rev. B **51**, 9271 (1995)
17. A.J. Millis, Phys. Rev. B **48**, 7183 (1993)
18. P. Monthoux and D. Pines, Phys. Rev. B **49**, 4261 (1994)
19. R. Preuss, W. Hanke, and W. von der Linden, Phys. Rev. Lett. **75**, 1344 (1995)
20. M. Rozenberg, G. Kotliar, H. Kalueter, G. A. Thomas, D. H. Rapkine, J. M. Honig, and P. Metcalf, Phys. Rev. Lett. **75**, 105 (1995)
21. S. Sachdev, A.V. Chubukov and A. Sokol, Phys. Rev. B **51**, 14874 (1995).
22. S. Sachdev and A. Georges, Phys. Rev. B **52**, 9520 (1995).
23. J.R.Schrieffer, X.G.Wen, and S.C.Zhang, Phys. Rev. B **39**, 11663 (1989).
24. J. R. Schrieffer, J. Low Temp. Phys. **99**, 397 (1995).
25. B. I. Shraiman and E.D. Siggia, Phys. Rev. Lett. **61**, 467 (1988).
26. X-G Wen and P.A. Lee, preprint.

## FIGURES

FIG. 1. (a) The chemical potential as a function of the coupling,  $g_e$ . We used (in units of  $t$ ),  $\delta = 0.1$ ,  $C = 0.3$ ,  $t' = -0.45$ ,  $x = 0.1$ . For free fermions,  $\mu = \mu_0 \approx -1.16$ . The arrow indicates the value of  $g_e^{(3)}$  when hole pockets are formed. (b) The area of the occupied states vs  $g_e$ . The dashed line is the area for free fermions.

FIG. 2. (a) - (f) Fermi surface evolution with increasing  $g_e$ . The parameters are the same as in Fig. 1. For these parameters,  $g_e^{(1)} = 0.21$ ,  $g_e^{(2)} = 0.3$ , and  $g_e^{(3)} \approx 0.82$ . The figures are for  $g_e = 0$ ,  $g_e = g_e^{(2)} > g_e^{(1)}$ ,  $g_e^{(3)} > g_e > g_e^{(2)}$ ,  $g_e \geq g_e^{(3)}$ ,  $g_e > g_e^{(3)}$ , and  $g_e \gg g_e^{(3)}$ , respectively. In (c), the nested pieces of the Fermi surface are shown in bold. In Fig. (e), we also presented the values of the quasiparticle residue along the Fermi surface.

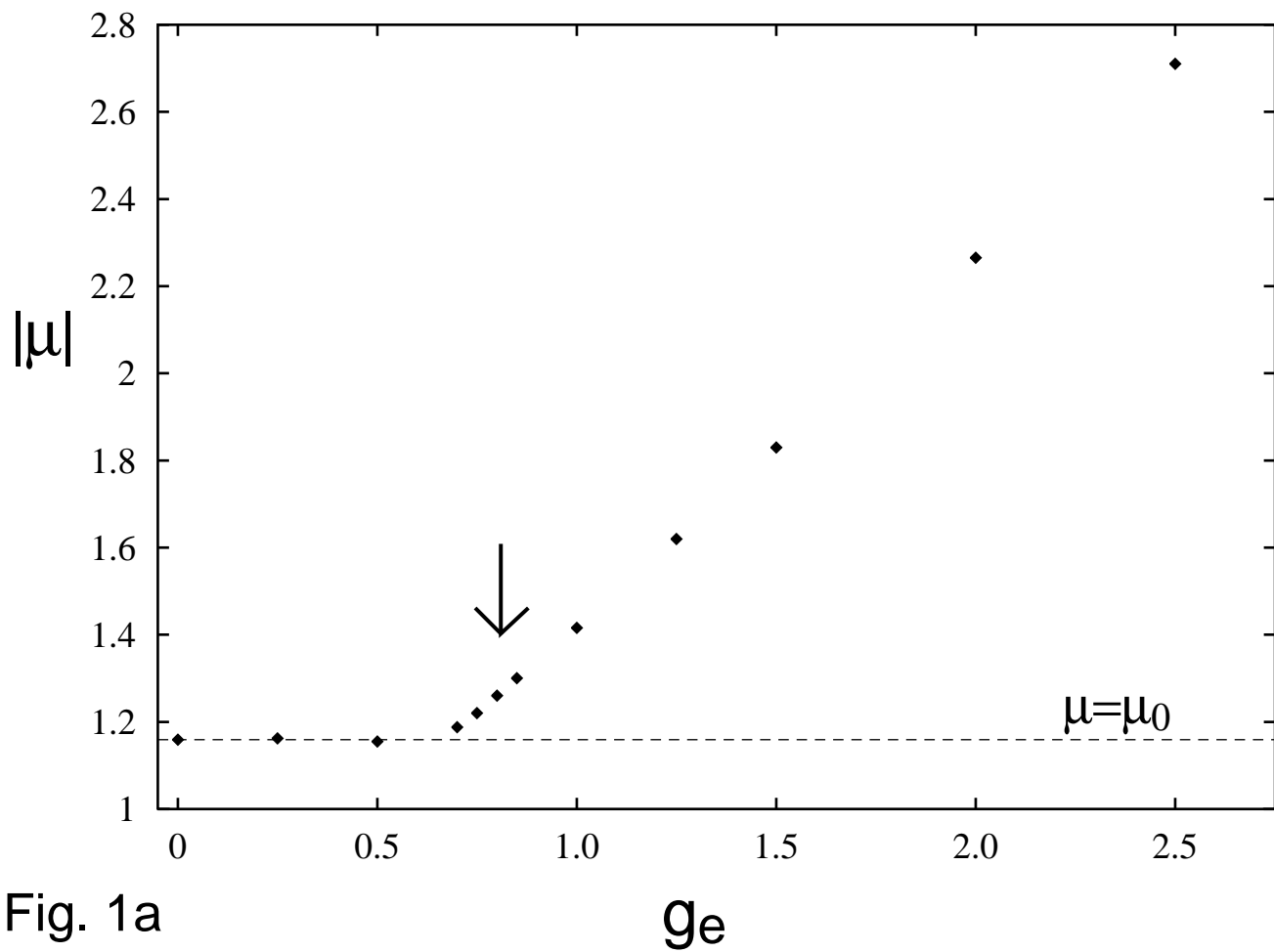


Fig. 1a

$g_e$

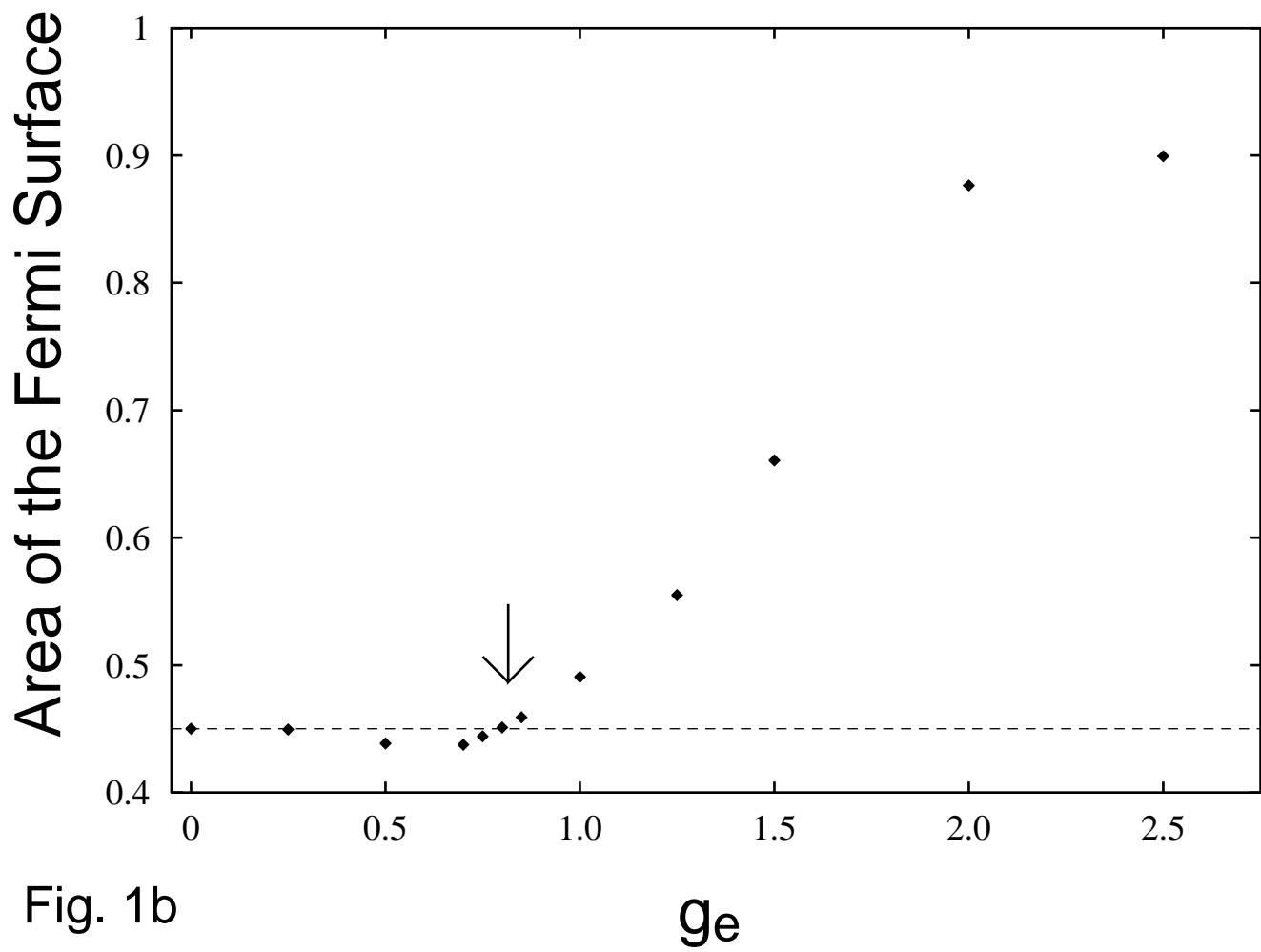
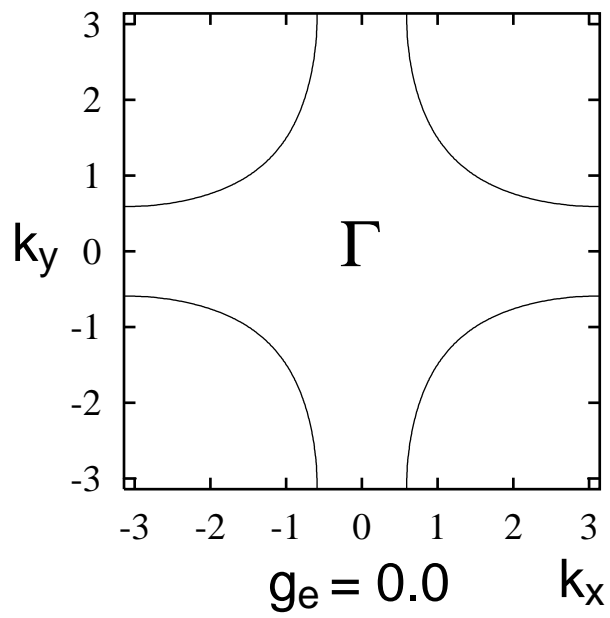


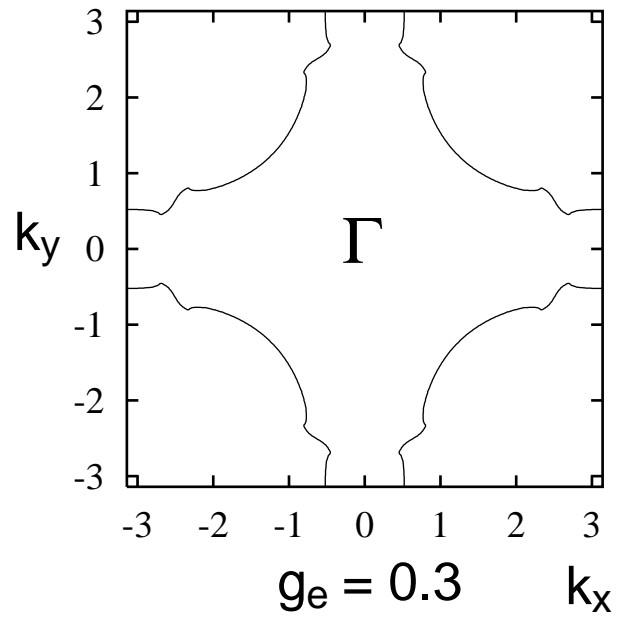
Fig. 1b

$g_e$

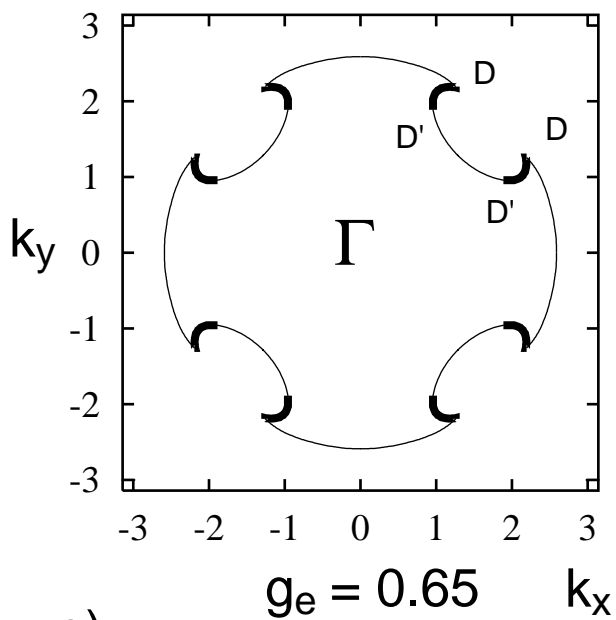
Fig. 2a)



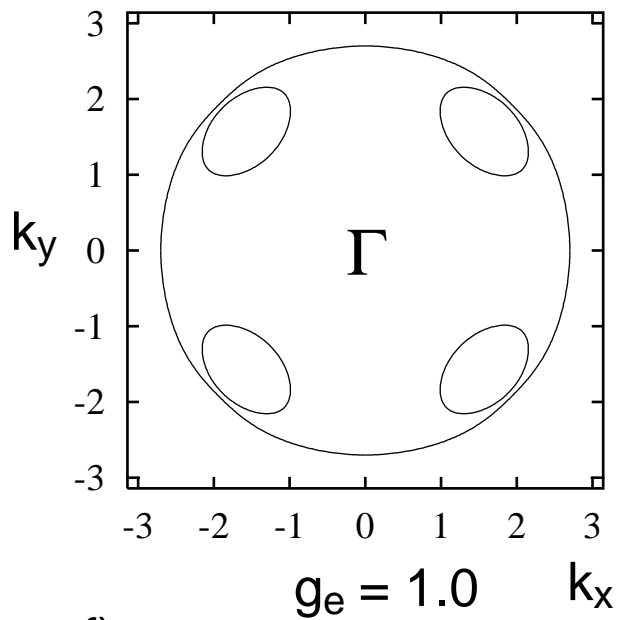
b)



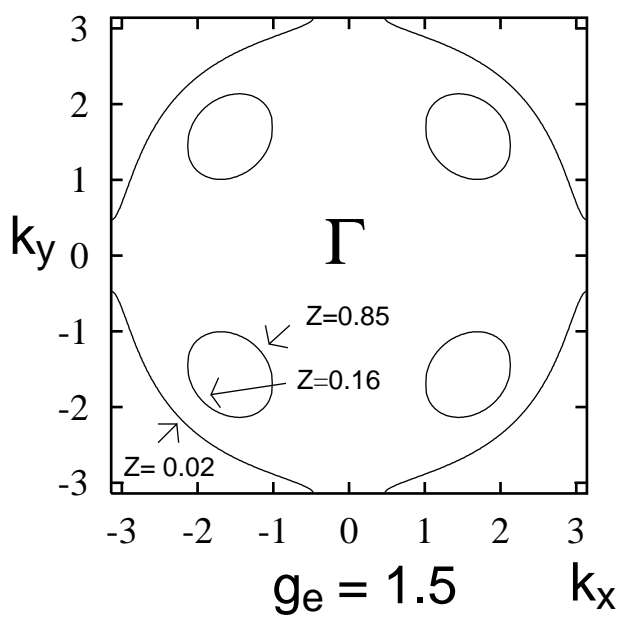
c)



d)



e)



f)

